A Methodology for Designing Light Hull Structure of Ice Class Vessels

MARINE 2021

Ruiz-Capel S. [1,*], Riska K. [2] and Gutiérrez-Romero J. E. [3]

[1,3] Escuela Técnica Superior de Ingeniería Naval y Oceánica (ETSINO), Universidad Politécnica de Cartagena (UPCT), Paseo Alfonso XIII, 52, 30203 Cartagena, Spain. Email: Jose.Gutierrez@upct.es web: http://www.navales.upct.es

[2] Norwegian University of Science and Technology (NTNU), Marine Technology Department, Otto Nielsens veg 10, 7491 Trondheim, Norway. Email: kaj.riska@welho.com

[*] Corresponding author: Ruiz-Capel S., samu_rcc@hotmail.com

ABSTRACT

Polar navigation requires more powerful ships with increased hull strengthening capable of overcoming the additional resistance presented by sea ice and able to withstand the impacts of the many ice formations that might appear. The increase in capability of a ship to overcome the resistance whilst moving through ice infested waters, plus the extra weight of its structure due to the higher strengthening, requires greater power. Consequently, the added requirements needed by ice-going vessels entail higher emissions of pollutants into the atmosphere, greater initial investment for shipbuilding and huge operational costs. Hull strengthening of ice class vessels is defined by a proper Classification Society in their rules, which trend towards conservative equations (TRAFI, 2016). This work describes a methodology to obtain lighter hull structures of polar vessels by using an impact model of a ship against an ice floe, based on energy methods, and focused on early stages of design (Popov *et al.* 1967; Daley 2001; Jumeau & Riska 2018). The hull structure of the bow region of an ice class ship is designed according to the Finnish-Swedish Ice Class Rules (TRAFI, 2016) and both results of the ship's bow weight calculated through direct calculation and current regulations are compared. Finally, some conclusions related with weight reduction are shown.

Keywords: weight optimization; hull strengthening; ice impact; FSICR; ice-going vessels; ship-ice interaction.

NOMENCLATURE

A	Contact area [m^2]
a	Length of a rectangular-plate panel [m]
B	Breadth [m]
b	Width of a rectangular-plate panel [m]
C	Geometry factor for the collision [-]
D	Depth [m]
d	Ice floe edge's deflection [m]
d_2	Ice floe width [m]
e	Width of a rectangular-load footprint, parallel to b [m]
F	Contact force [MN]
$F_{\max}$	Maximum contact force [MN]
f	Length of a rectangular-load footprint, parallel to a [m]
H	Height of the load patch [m]
H_1	Load height for a rectangular uniformly partially distributed load [m]
H_2	Load height for a triangular partially distributed varying load [m]
h_f	Width of the profile's flange [mm]
h_w	Height of the profile's web [mm]

h_2	Ice floe thickness [m]
L	Frame span [m]
L_{pp}	Length between perpendiculars [m]
L_2	Ice floe length [m]
L_3	Application point of the ice load [m]
L_4	Initial point of the ice load [m]
M_{avg}	Maximum bending moment on an averaged frame fixed at both ends and simply
M_{max}	Maximum bending moment on a simply supported frame [N m]
M_{max1}	Maximum bending moment on a frame with rectangular uniformly partially distributed load [N m]
M_{max2}	Maximum bending moment on a frame with triangular partially distributed varying load [N m]
$M_{\text{max}}{}'$	Maximum bending moment on a frame fixed at both ends [N m] supported [N m]
n	Pressure-area exponent [-]
P	Ice load [MPa]
P_0	Nominal, peak or average ice pressure [MPa]
s	Frame spacing [m]
T	Draught [m]
TOW	Total weight of the bow region of a vessel design [t]
$TW_{\text{b profiles}}$	Total weight of the bulb flat profiles [t]
$TW_{\text{L profiles}}$	Total weight of the angle profiles [t]
TW_{plate}	Total weight of the shell plate [t]
$TW_{\text{stringers}}$	Total weight of the ice stringers [t]
$TW_{\text{T profiles}}$	Total weight of the custom-built T profiles [t]
t_f	Thickness of the profile's flange [mm]
t_s	Thickness of the shell plate [mm]
t_w	Thickness of the profile's web [mm]
v_{ice}	Ice floe velocity [m s^{-1}]
v_1	Ship velocity [m s^{-1}]
W	Width of the load patch [m]
w_1	Width of the load patch smaller than s [m]
w_2	Width of the load patch equal to s [m]
w_3	Width of the load patch bigger than s [m]
x_b	Displacement due to bending of the ice floe [m]
x_{cr}	Displacement due to crushing of the ice floe [m]
x_1	Movement of the ice floe produced by the displacement of the ship [m]
x_2	Displacement due to the translation of the ice floe [m]
Z	Section modulus [m^3]
α	Waterline angle [°]
β	Frame angle [°]
β'	Normal frame angle [°]
γ	Sheer angle [°]
Δ	Displacement [t]
δ	Ice-edge opening angle [°]
σ_{ris}	Required yield stress [MPa]
φ	Buttock angle [°]
ψ	Flare angle [°]
FSICR	Finish-Swedish Ice Class Rules
IACS	International Association of Classification Societies
IMO	International Maritime Organization
LIWL	Lower Ice Waterline

M/S	Motor Ship
RMRS	Russian Maritime Register of Shipping
STA	Swedish Transport Agency
TRAFI	Finish Transport Safety Agency
UIWL	Upper Ice Waterline
WARC	Wärtsilä Arctic Research Centre
WMO	World Meteorological Organization
(b)	Bulb flat profile
(T)	Custom-built T profile
(L)	Angle profile

1. INTRODUCTION

As ships navigate through northernmost or southernmost routes, they reach latitudes where additional hazards, notably sea ice, may have to be overcome. Sea ice is any form of ice found at sea which has originated from the freezing of sea water. Many forms of sea ice can be presented depending on size, origin, concentration, age, stage of development, etc. These forms give a wide number of different definitions for sea ice defined by the World Meteorological Organization (WMO, 2014). If sea ice impacts a vessel navigating in ice covered waters, it can cause severe damage to the structure of the ship.

In order to avoid damage to the hull, ice-going vessels must be designed according to existing rules whose aim is to provide safe ship operation and protection of the polar environment by addressing the risks presented in polar waters. The risks of navigating ice infested waters under extreme climate conditions are wider than only the impact of ice itself: topside icing, the congealing of fluids in different systems due to low temperatures and the inexperience of crew members in polar waters among others. These hazards necessitate special requirements regarding the ship's structure, power, subdivision and stability, hull strengthening and considerations concerning equipment and navigation among others. These requirements are detailed in the Polar Code (IMO, 2014).

The construction of polar class ships must be in accordance with certain special sets of rules that define the required features of ice capable vessels. The creation of these regulations is based on the experience gained throughout the years by studying ice model tests, ice navigation features and damage to ships when navigating through ice. The impact produced by level ice is not usually a risk, since its thickness and properties are included in the design rules. However, risk may be presented when occasionally hitting undetected larger ice floes. Aiming to obtain an adequate approach to the forces exerted by the ice on the hull of ice capable vessels, some models have been developed for the impact between ship and ice. These models are used to estimate the ice loads on different structural elements of a ship and to determine the required thicknesses and structural configuration, which can be used as a basis for the development of the ice class rules or direct design.

Popov *et al.* (1967) developed a model which set the basis for the ice class rules of the Russian Maritime Register of Shipping (2016) (RMRS). Popov's model is used for obtaining ice loads acting on the side of a ship's hull whilst sailing in ice. Some assumptions are made for the ship and floe in order to simplify the model, such as the ship being symmetric with respect to its centreline and the ice floe being round in shape.

The complexity of crushing prompted researchers to devise new tests in order to understand the ice crushing process. Crushing is understood as a non-continuous process including elastic contact, damage to the solid, fracture, re-breaking of trapped ice, and extrusion of granular material. Joensuu & Riska (1989) conducted experimental tests for crushing in Helsinki, at Wärtsilä Arctic Research Centre (WARC) in 1988. As results of these tests, they observed that the ice in contact with the indenter was thin and line-like. They also noticed that the recorded signal had triangular peaks that grew in size when the indentation increased. Daley (1991) created a simple model for crushing that was able to reproduce most of the results obtained by Joensuu & Riska (1989). His model treated ice edge failure as a hierarchy of failures, each being superseded by the failure of the supporting mechanism and did not contain extrusion considerations.

Daley (1999, 2001) proposed an energy-based collision method for different ice floe shapes and impact types (shoulder, head-on). The method is based on Popov's energy method, introducing the concept of pressure-area relationship for the indentation in the ice. Other models have been proposed for impact of a ship against ice (Daley & Kim 2010; Bueno 2012; Dolny 2018).

The risk of damage to a polar vessel when impacting a large ice floe is reduced by increasing the strengthening of the hull through augmented thicknesses for their structural elements according to a proper ice class. Ice class regulations tend to be quite conservative at the moment of assigning hull scantlings. This may turn into an excessive increase of steel weight and, consequently, rising pollutant emissions and operational and constructive costs. The present paper aims to present a methodology to reduce the weight of this kind of vessels through a direct calculation method.

The second section of the article presents a method for hull scantlings calculation for a sample vessel, through one of the most popular ice class regulations: The Finnish-Swedish Ice Class Rules (FSICR). Next, section 3 describes a method proposed to estimate the hull scantlings of a vessel by means of direct calculation based on Popov's *et al.* (1967) model and the load patch concept. By using this method, the hull scantlings for the sample vessel are recalculated and the weight of multiple designs is obtained and compared to that estimated by means of the FSICR, whose results are shown in section 4. Finally, the conclusions for this work are shown in the last section of this article.

2. HULL SCANTLING THROUGH ICE CLASS REGULATIONS

The oldest regulations concerning navigation through ice infested waters, 'The Imperial Statutes', were developed by Finland in 1890, (Finland being a part of Russia at the time). Initially, they were only a set of recommendations related to the construction and fitting out of ships for winter navigation. Since the development of the rules, they have included some updates. In 1920 the first Finish ice class rules for shipping were created in which scantlings were set as some relative increase in the open water scantlings. Later, in 1932, three ice classes were introduced (IA, IB, IC) as well as ice class II corresponding to open water ships and ice class III corresponding to barges. The next significant change came in 1965, with the introduction of the ice class IA Super. After having noticed that the strengthening for these ships was too weak based on the evidence of damage caused to ships, a large ice damage survey was carried out. As a result, Finland and Sweden made an agreement and jointly developed the Finish-Swedish Ice Class Rules in 1971, in order to give adequate strengthening to ice-going ships and to manage the maritime traffic in winter. In 1985, the hull rules changed with the introduction of a new idea relating to ice load height. The ice performance requirement changed in 2002, requiring a minimum speed of 5 knots in a brash channel according to the design class. In 2006 the rules were updated with regard to the ice waterlines and in 2008 new machinery rules were introduced. The rules were updated in 2010 in order to streamline the hull rules. The latest update of the rules was made in 2017, to include new azimuthing requirements for operating in ice (TRAFI 2016; Riska & Kämäräinen 2011). The FSICR has been selected to address a hull scantling calculation through ice class regulations for weight estimation.

Experiences of winter navigation in the Baltic Sea have been collected throughout the years and safety measures and knowledge have been consequently adopted, as it is presented in the rules document 'Ice Class Regulations and the Application Thereof', published by the Finnish Transport Safety Agency (TRAFI, Finland) and the Swedish Transport Agency (STA, Sweden). They have 6 different ice classes defined as ice class III, II, IC, IB, IA and IA Super, in order of increased strengthening. The hull strengthening is divided into 3 main regions (bow, mid-body, aft) and 2 subareas within the bow region (fore foot and upper bow ice belt), as shown in Figure 1.

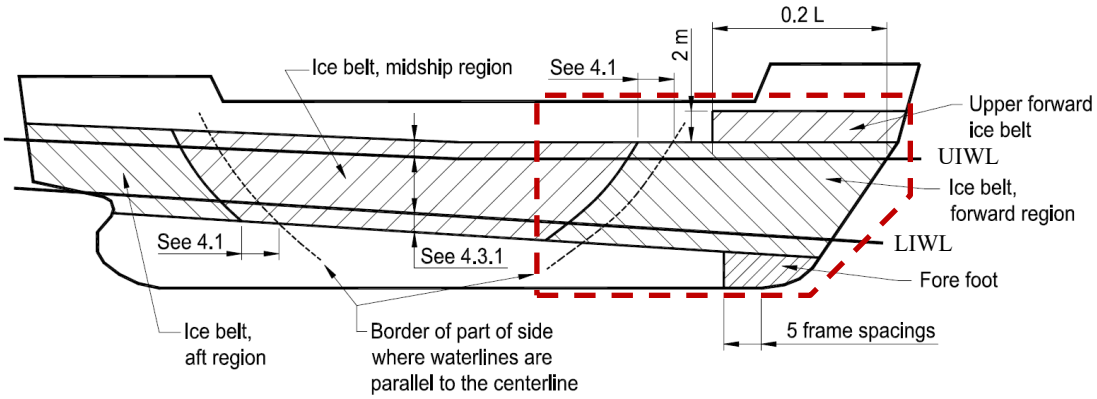

Figure 1: Different regions for the ice strengthening defined by the FSICR (TRAFI, 2016). The red box indicates the bow region, which is the area of the vessel to be studied in this work.

For the sake of later comparison with the direct calculation method and for simplicity, only the bow region is considered in the calculations of hull scantlings. Once the engine output and the ice load for the selected ice class are known, the ice pressures applied to the hull produced by a ship of certain features and power are determined. With the ice loads applied to each single member of the hull (plate, frames, stringers and web frames) the whole ship's scantlings can be calculated, the weight of the bow region being estimated.

In order to give an approach of the calculation of the weight in the bow region through the FSICR to be further compared to the weight calculated by means of the direct calculation method, a case study has been used. The sample vessel used for this research is the bulk-carrier M/S Eira, a vessel of the company ESL Shipping (2020), shown in Figure 2. This vessel was built in 2001 by Tsuneishi Shipbuilding Co. Ltd, Japan, and currently sails under the flag of Finland for bulk trading between Nordic Countries. The vessel was classified by the Classification Society Lloyd's Register and was built to comply with the ice class IA Super of the Finnish-Swedish Ice Class Rules. The engine output and hull scantlings have been recalculated for the vessel, according to the real structural distribution of its members ($s = 0.4$ m, $L = 2$ m). The recalculated engine output used for the hull scantling is superior to the actual engine installed on the ship, due to a change in this part of the rules. The value used for the engine output is 10470 kW.

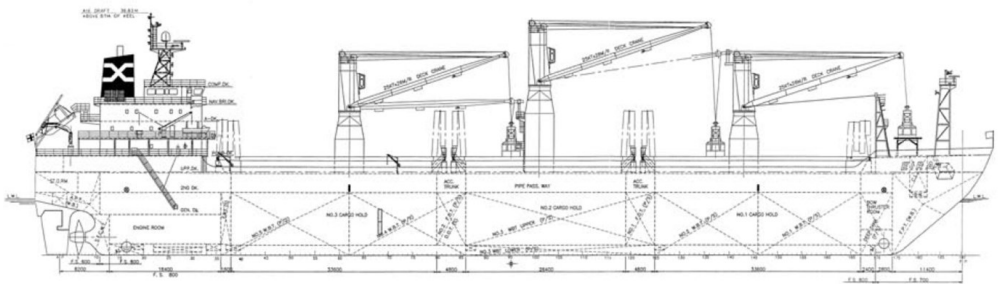

Figure 2: General arrangement of the profile of the 'M/S EIRA' (Jumeau & Riska, 2018).

Table 1: Parameters of the 'M/S EIRA' (adapted from Jumeau & Riska 2018; ESL Shipping 2020).

Length between perpendiculars	L_{pp}	148.00 m
Breadth	B	24.60 m
Draught	T	9.03 m
Depth	D	13.00 m
Displacement	Δ	26000 t

3. DIRECT CALCULATION METHOD

The direct calculation is addressed to obtain an estimation of the hull scantlings of the sample vessel, their weight being compared to that obtained through the FSICR.

3.1 Impact Model

The model of impact between an ice floe against a ship's hull to ascertain a direct calculation method of the collision force and the ice load on frames and plating on the selected ship has been developed by Jumeau & Riska (2018). The model is based on an energy method model initially developed by Popov *et al.* (1967), including the idea of load patch extracted from the conclusions of Joensuu & Riska (1989) and the concept of pressure-area relationship developed by authors such as Sanderson (1988). The crushing depth is calculated by using a Lagrangian approach. The model is developed for oblique or shoulder collision, that is, an impact on the bow, on a side of the ship's hull, where ice can impact a frame directly.

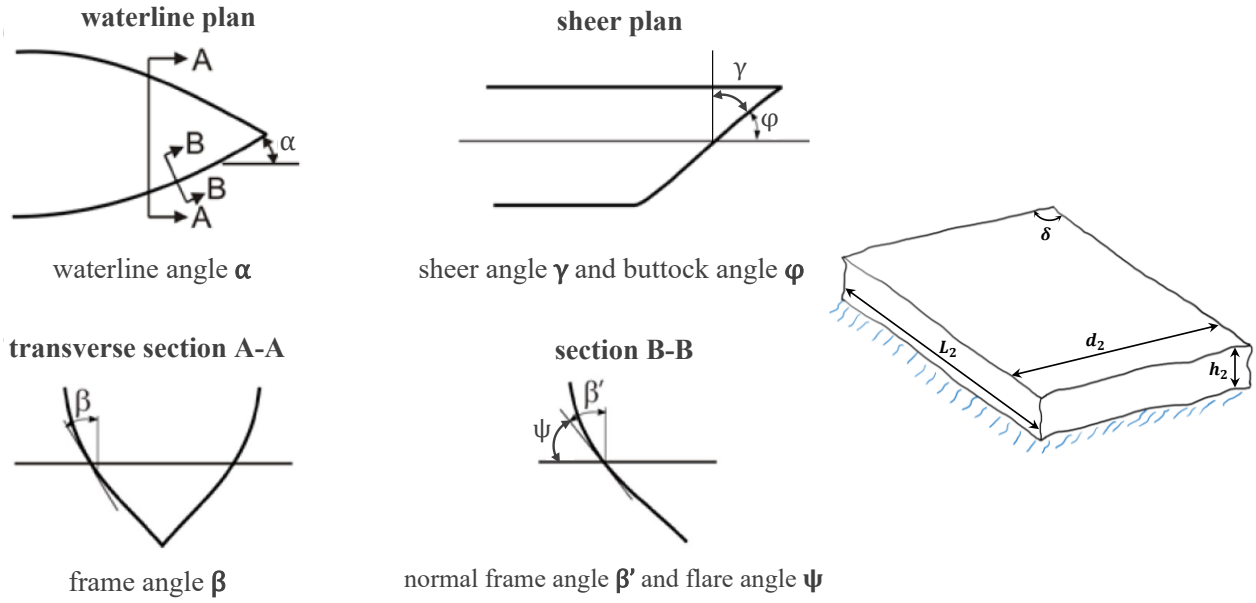

Figure 3: Left: Hull angles definition, unified from IACS, Daley (1999, 2001) and the FSICR (TRAFI, 2016). Right: Definition of main dimensions of the sample ice floe. The ice floe considered for the impact model is rectangular shape, its size being 20 m in length, 10 m wide and thickness of 1 m (adapted from Jumeau & Riska, 2018).

In order to simplify the calculation of the contact force, different assumptions are included in the model, similar to those for the model of Popov *et al.* (1967) for a round ice floe. In this case, the ice floe is rectangular wedge-edged shaped and relatively small in comparison with the ship. The ship is considered to be a rigid solid body. During the impact, hydrostatic and hydrodynamic forces resulting from the translation of the ship and the ice floe are assumed to be small compared to the contact force (F). Before the impact, the ship is moving at a speed v_1 in positive direction of the X axis and the ice floe remains immobile ($v_{\text{ice}} = 0$). The influence of frictional forces on the value of the ice loads is relatively small. Therefore, frictional forces are disregarded. Sliding is not considered in the model.

The process of collision includes several displacements originated by different phenomena. For the sake of simplicity, the three-dimensional (3D) model is reduced into a one-dimensional (1D) system considered as a line normal to the impact's direction on the hull (see Figure 4). The movement of the ice floe produced by the displacement of the ship (x_1) in the direction of the impact is then divided into the sum of the translation of the ice floe (x_2), the displacement due to crushing (x_{cr}) and due to bending (x_b).

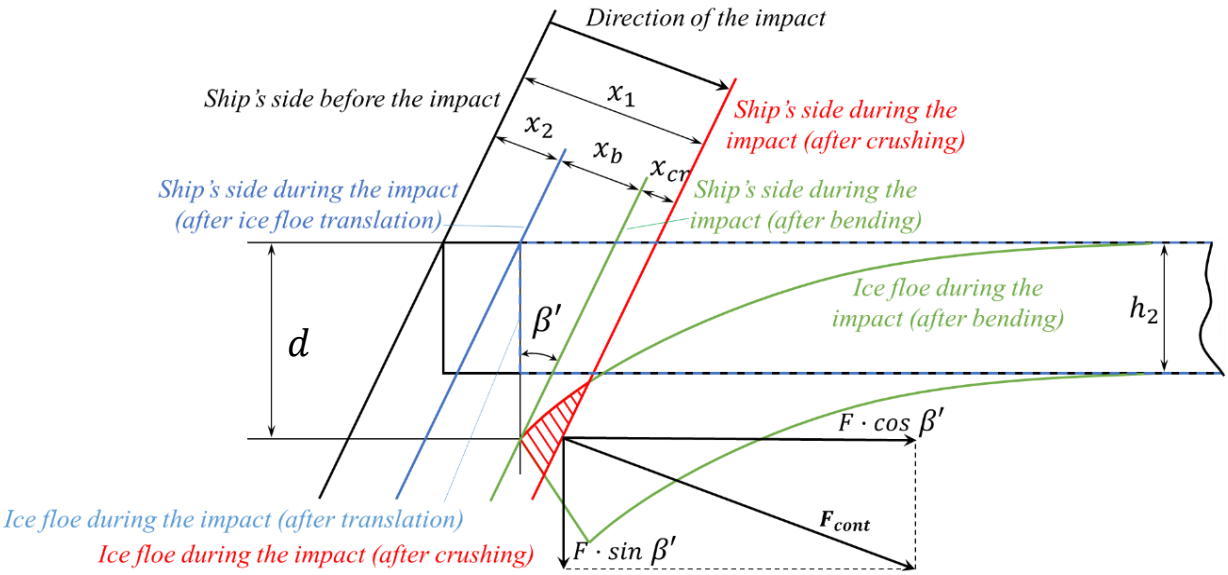

Figure 4: Diagram of impact taking translation, crushing and bending into account. Cross section of the ship and the ice floe with a vertical plane containing the hull's normal vector (adapted from Popov *et al.* 1967).

The definition of the contact force, according to Jumeau & Riska (2018) is

$$F = \int_0^A P \cdot dA = P \cdot A, \tag{1}$$

substituting the pressure area relationship, it being $P = P_0 \cdot A^n$, the formula for the contact force is

$$F = P_0 \cdot C^{n+1} \cdot {x_{cr}}^{2n+2}, \tag{2}$$

where P_0 is the average or nominal pressure, n is the pressure-area exponent and C is a geometry factor.

This model does not consider the breaking of the ice floe. Therefore, it is valid when the bending force is not greater than force needed by the ice floe to break, that is, the fracture force. The velocity of the ship is assumed to be 5 knots for the impact, same as appointed by the FSICR for direct calculation.

3.2 Frame Formulation

When applying the model of impact between the sample ship and the sample ice floe, the maximum contact force is derived. This value of the contact force is used to calculate the maximum stress on the hull structural members. The value of the maximum bending moment generated in beams and that of the section moduli (Z) of the profiles to use in the shipbuilding are obtained in order to further calculate the required yield stress.

Due to the nature of the loads produced when a ship is sailing in ice and the need of weight saving, most ice-going ships are built with the transverse framing system. The risk of hitting ice is mainly localized in the bow and sides of the ship, within the ice belt. Here, the highest loads are registered on the frames more so than on the plating, the transverse frames being the weakest members of the structure. The ice stringers, distributed along the depth of the ship, are less likely to be hit. Thus, the study of the ice load is centred on the ice frames. When the side of the vessel's hull impacts a piece of parallelepiped floating ice, the crushing process leaves a triangular area on the ice's corner dependent on the geometry properties of the two bodies. This triangular footprint is also the area of the load patch on the hull.

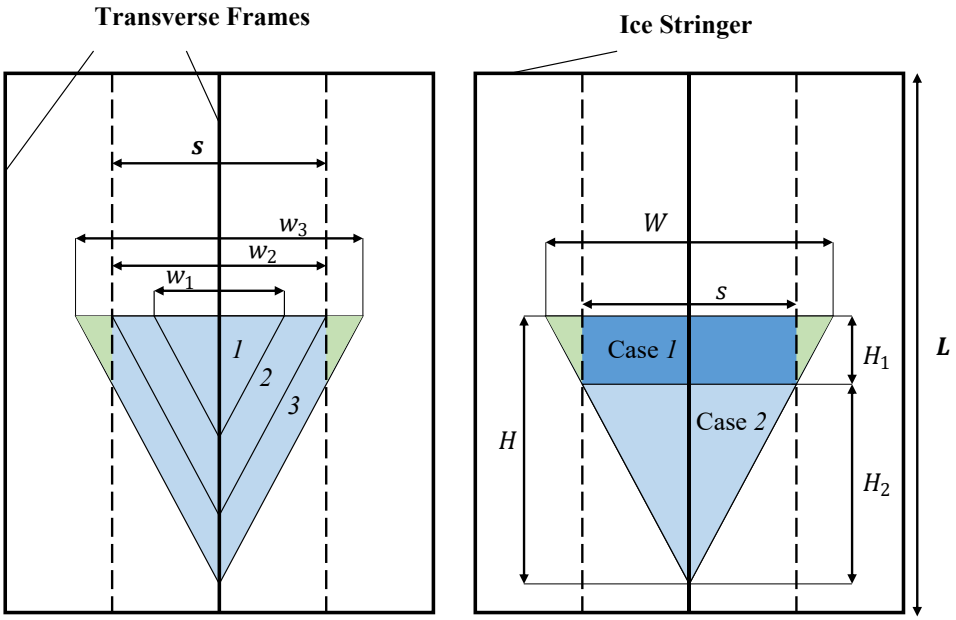

Figure 5: Left: Ice load patch configuration, the width of the load patch area being in the direction of the ship's length and its height in the direction of the ship's depth. Evolution over time of the load patch: 1) Load patch when $w < s$; 2) Load patch when $w = s$; 3) Load patch when $w > s$; Right: Load division in two cases when the framing configuration allows a load patch area 3: case 1) rectangular load, green triangles are excluded and its load is supported by the next frame; case 2) Triangular load (adapted from Jumeau & Riska, 2018).

Depending on the configuration of the frames (frame spacing), the evolution of the load patch over time can diverge into two different situations, in terms of supported load patch area by a single frame. The ice load is assumed to be applied directly to the frame, the frame being the symmetrical axis of the load patch area (see Figure 5, left). If the selected configuration of the ship's structural members allows large enough frame spacing, the load patch area (1) is always within the space between two transverse frames (s), thus the width (horizontal base of the triangle) of its footprint (w_1) is never bigger than the frame spacing (s). In this situation, the whole impact load is supported by the single frame and the load patch has dimensions W, H in triangular shape, according to the previous definition in Figure 5.

On the other hand, if the configuration for framing implies that the frames are too closely distributed, the ice load starts growing with area 1, the width of the load patch area (w_1) being smaller than the frame spacing (s). As time continues, the load patch area grows until the moment in which its width (w_2) reaches the size of the frame spacing (maximum triangular area supported by a single frame, area 2). With the increasing load, the width of the triangle (w_3) comes to a value larger than the distance between two frames and the loaded area is also shared between the adjacent frames (small green, triangular area in the figure above, area 3). In this situation, the load patch area supported by the single frame is the sum of a rectangle (case 1) and a triangle (case 2).

The frames on a ship welded to the shell plate can be presented in multiple ways, their ends being welded to the supporting frames or crossing them, and with or without brackets. The installation mode of these frames can give higher or lower stiffness to the bar-system, allowing different movements and restrictions. The use of the beam theory to approach the frames is not an exact solution in reality, but gives a good approximation to it. For this reason, the beam theory is used to determine the bending moments produced by the ice load applied on a frame. In order to include the possible differences presented in reality, the frame is approached as a simply supported beam and as a beam fixed at both ends.

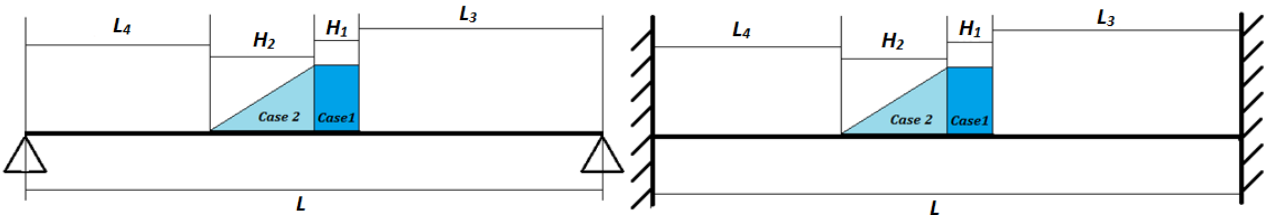

Figure 6: Ice load distribution on a simply supported frame (left) and on a fixed frame at both ends (right) when the horizontal dimension of the load patch area is greater than the frame spacing (adapted from Jumeau & Riska, 2018).

Ice loads presented in Figure 6 correspond to a rectangular uniformly partially distributed load (part of the contact area greater than the supported area by a single frame, case 1) and a triangular partially distributed varying load (part of the contact area smaller than the supported area by a single frame, case 2). The total length of the frame (L) or frame span is then considered as the sum of the length of application of the rectangular load (case 1) and the triangular load (case 2), the distance between the beginning of the beam and the initial point of the load (L_4) and the distance from the end of the load to the end of the beam (L_3). The application point of the ice load is defined by the distance L_3. The maximum bending moment ($M_{\max 1}, M_{\max 2}$) is then calculated for these two cases. Assuming small and linear deformations, the superposition principle can be applied: the total maximum bending moment ($M_{\max}$) for a simply supported frame is the sum of them both,

$$M_{\max} = M_{\max 1} + M_{\max 2} \tag{3}$$

The framing system of a ship can be accomplished by using several types of frames. Each profile type has a different capability to resist loads on structures depending on their shapes, which determine their capacity to withstand shear forces and loads through proper shear areas and section moduli (Z). This profile shape also affects the total weight of the profile and thus, the weight of the whole ship. For this case, bulb flat, angles (L) and T profiles have been selected for the optimization process in hull's weight, since they are some of the most frequently used types in the shipbuilding industry. The profiles are differentiated into commercial bulb flat and L profiles by buying standard profiles, and custom-built T profiles which are manufactured in the shipyard. This differentiation is made with the aim of optimizing the individual thickness and height of T profiles, since they can be custom-built to the desired dimensions.

Once the maximum bending moment on a frame ($M_{\max}$) and the elastic section modulus (Z) of a frame and its associated plate are calculated, the required yield stress of the material used to build the frames (σ_{ris}) which have to withstand $M_{\max}$ can be obtained.

3.3 Shell Plating

When navigating in ice infested waters, the risk of structural damage due to ice impact not only affects the transverse frames. It is actually possible that the ice hits the ship in the middle of a panel of the shell plating. This scenario has been considered for the estimation of the hull plate scantling.

Single location loads are loads expected to occur rarely and are considered to occur in the centre of the panel, where the bending moment is the maximum (Hughes & Paik, 2010). Ice impacts can be considered as accidental loads, since collision is intended to be avoided when navigating in ice. This theory for concentrated loads, developed by Hughes & Paik (2010), has been used to estimate the plate thickness. As explained for the frame formulation, the load patch is triangular shape, thus the loaded area within two frames varies depending on the structural configuration, as shown in Figure 7. Due to the fact that the load area defined for the single location loads theory is rectangular shaped, a transformation of this triangular footprint into a rectangular one is made.

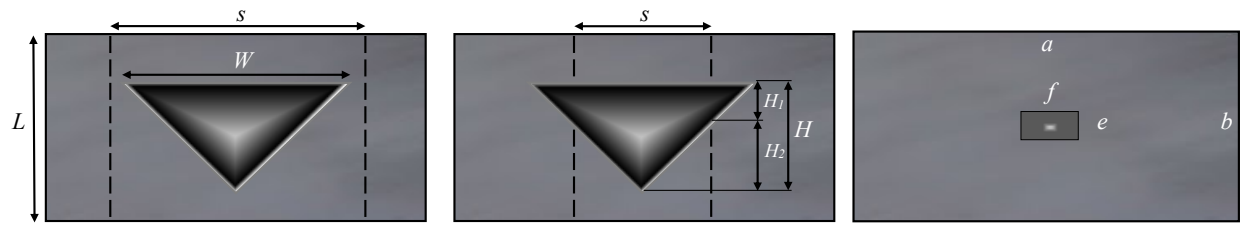

Figure 7: Load patch on the shell plate due to impact against a wedge-shaped ice floe. Left: when the frame spacing is larger than the width of the load patch $W < s$. Middle: when the frame spacing is smaller than the width of the load patch $W > s$. Right: Parameters definition for a panel and the footprint created by a partially concentrated load, according to Hughes & Paik (2010).

3.4 Optimization Process

The input data for the optimization process are obtained from the parameters corresponding to the ship features, the ice floe, and those that are necessary to obtain the contact force. Once the problem is defined, the in-house code is run to obtain the contact force ($F_{\max}$). This force is the ice load to be applied for the calculation of the shell plate thickness and the maximum bending moment produced on a frame for a simply supported frame ($M_{\max}$), fixed frame ($M_{\max}{}'$) and the average of them both (M_{avg}). With the bending moment and the shell plate thickness, the modulus of the frame and its associated plate can be calculated. Three types of profiles are then used, and their moduli are to be obtained, changing the profile size (for standard profiles) or parameters which define the profile (for custom-built profiles). The number of total designs to be considered in the optimization process depends on the selected range of these parameters of the profile and the number of profiles for each type, together with the number of configurations for the stiffeners, that is, the distribution of frames and stringers to study.

The weight for each of them is estimated according to the configuration, frame type and size of every design. Since the bending moment and section modulus are also calculated, the required yield stress of the material to use in building that ship design is obtained. Each case is plotted on a graph representing required yield stress-weight, and the lightest designs which do not exceed the actual yield stress of the steel used in the ship (355 MPa) are selected and pointed in the Pareto front. Then, all the futures of the selected designs are extracted, having different ships with certain total weight (TOW), structural configuration (s, L), shell plate thickness ($\mathrm{t_s}$), profile type (bulb flat, L or T) and size (t_w and h_w of the profile). The optimization process is shown in Figure 8.

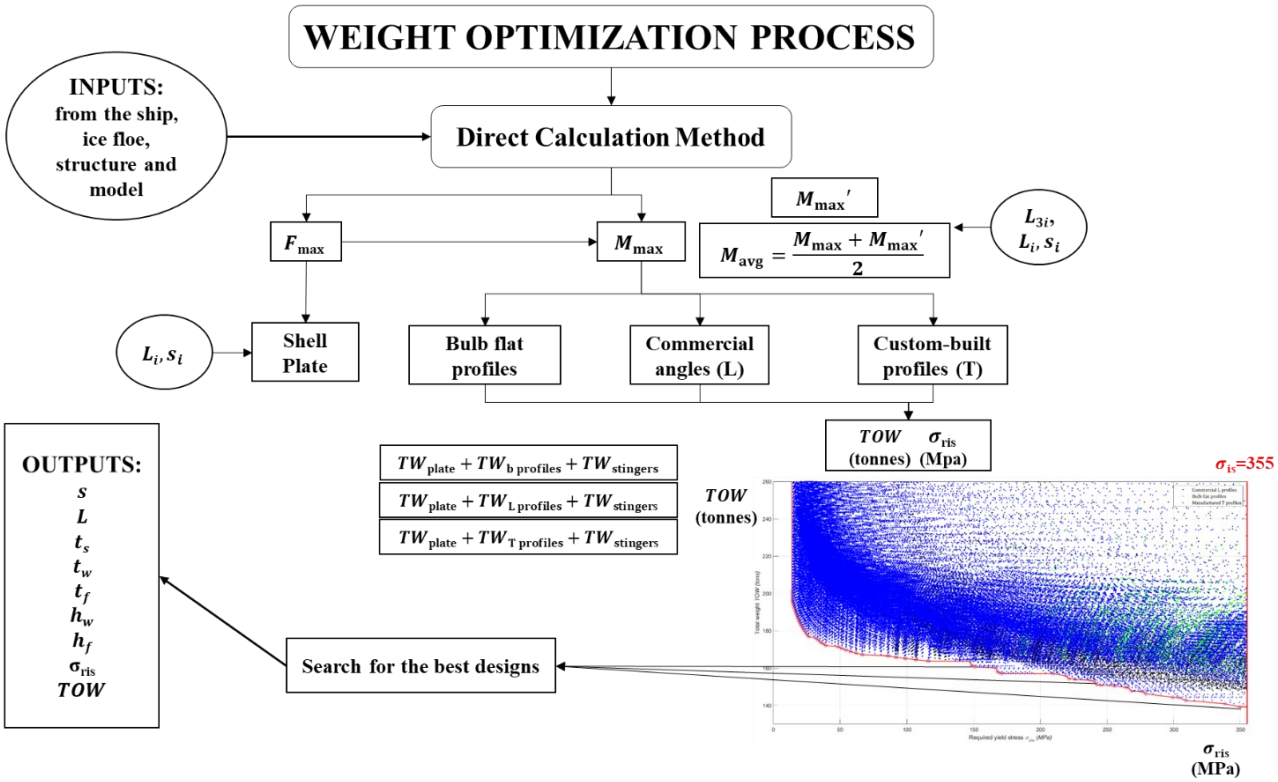

Figure 8: Overview of the performance for the process of hull's weight optimization.

4. RESULTS

The frame type used to determine the hull scantling through the FSICR is T profile, in order to simplify the calculation and maximize the weight reduction. Aiming at reducing the number of assessed designs through the direct calculation method, for T profiles, the thickness of the flange is taken to be the same as that of the web, its width being half that the web's height. The same assumption is taken for the hull scantling calculation through the FSICR.

Table 2 shows the hull scantlings calculated through the FSICR, obtaining the values for the dimensions of T profiles estimated for the different structural members. For simplicity, the curvature of the ship's side has been neglected when estimating the weight of these structural members. Once the weight of all these elements is estimated, the total weight of the steel used for the bow region is calculated.

Table 2: Hull scantlings obtained through the FSICR.

	Shell (mm)	**Transverse frames (mm)**				**Ice stringer (mm)**				**Web frames (mm)**				**Total weight, design (tonnes)**
	t_s	t_w	h_w	t_f	h_f	t_w	h_w	t_f	h_f	t_w	h_w	t_f	h_f	
	22	10	225	10	112.5	20	300	20	150	22	850	22	425	
Total weight (tonnes)	111.14	41.38				17.49				63.06				233.064

t_s = Thickness of the shell plate; t_w = Thickness of the profile's web; h_w = Height of the profile's web; t_f = Thickness of the profile's flange; h_f = Width of the profile's flange.

Figure 8 shows the design space with all the feasible designs calculated through the direct calculation method. Y-axis shows the total weight of the bow region for those designs, and the required yield stress of the profiles used to build those designs is shown in the X-axis. Each point on the graph is a unique design, it being built with custom-built T profiles (blue), bulb flat (black) or angle (green) profiles. All these designs are lighter than the design calculated through the FSCIR and have been built with profiles which require steel with yield stress of 355 MPa or less. Amongst them, optimal designs (red circles) are found in the Pareto front (red line), which are the lightest and most-resistant designs.

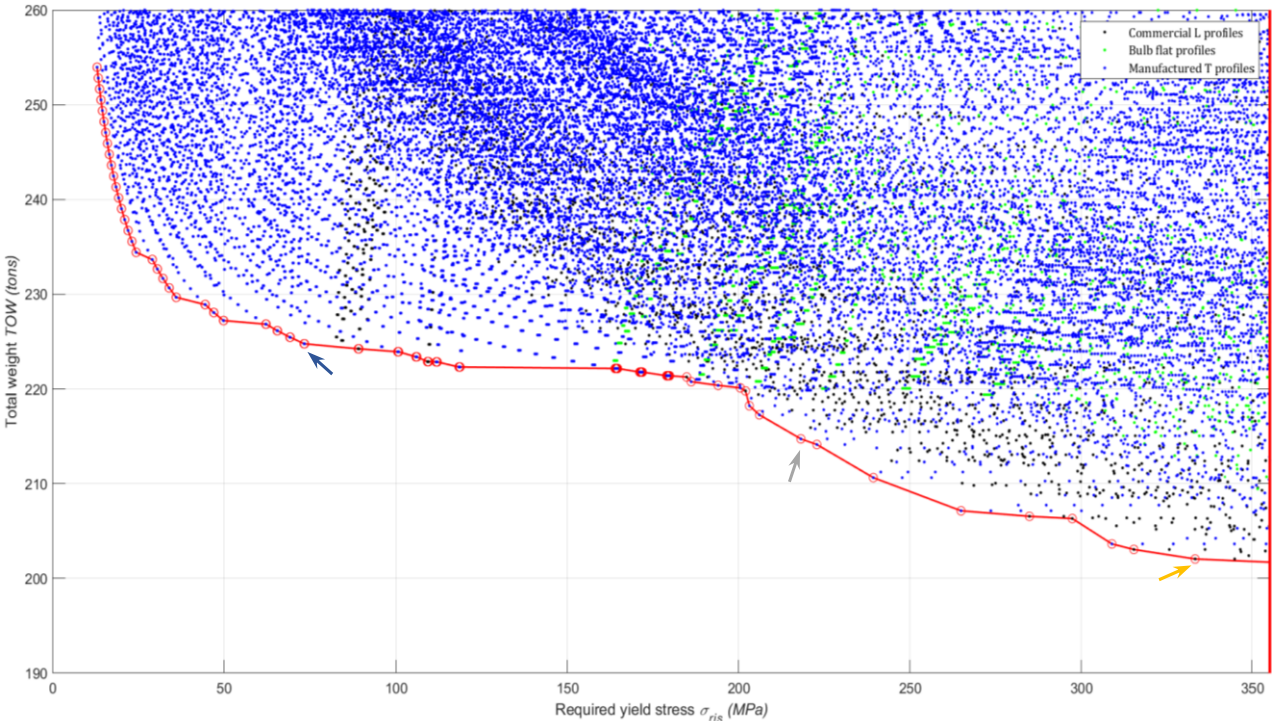

Figure 8: Pareto front on the feasible designs using averaged maximum bending moments. The three selected designs are pointed on the Pareto front (Design 1: orange = lightest design; Design 2: grey = light-resistant design; Design 3: purple = most-resistant design).

The features of five designs estimated under the three studied assumptions of supporting system are shown in Table 3. These designs correspond with the lightest design (1), the most-resistant design within the lightest designs (3) and one in-between (2). Since most designs are built with T profiles, the lightest design built with the rest of profile types are also shown, even though some of them are not found in the Pareto front.

Table 3: Features of the designs obtained through the direct calculation method.

	M_{max} (mm)						M_{max}' (mm)						M_{avg} (mm)					
Design	t_s	t_w	h_w	s (m)	L (m)	TOW (tonnes)	t_s	t_w	h_w	s (m)	L (m)	TOW (tonnes)	t_s	t_w	h_w	s (m)	L (m)	TOW (tonnes)
1 (T)	26	12	250	0.5	1.5	199.96	26	12	350	0.5	3.3	200.14	26	12	320	0.5	1.9	202.05
2 (T)	26	12	350	0.5	1.7	214.13	28	13	450	0.6	3.3	220.18	28	13	350	0.6	1.9	214.72
3 (T)	34	16	350	4	1	223.32	34	16	550	3.6	1	227.22	34	16	450	3.6	1	224.76
4 (b)	26	12	280	0.5	1.5	200.44	28	13	370	0.6	3.3	205.42	26	12	320	0.5	1.9	202.05
5 (L)	28	16	200	0.6	1.9	209.46	31	20	200	0.8	1.9	219.32	31	16	200	0.8	1.9	210.72

(T) = Custom-built T profile; (b) = Bulb flat profile; (L) = Angle (L) profile. Designs 1, 2, and 3: according to figure 8. Designs 4 and 5: the lightest of its kind of profile.

5. CONCLUSIONS

Vessels navigating in polar waters require both high power and strengthened hulls, the goal of this research being to obtain a weight reduction for the strengthening of the hull structure. In this way, the additional weight required by hull strengthening is reduced through the application of a direct calculation method assuming impact with an ice floe.

The required yield stress of the material to build each design is calculated with the maximum bending moment and the section modulus of the profile used. This optimization process consists in checking which ones of the assessed designs are the lightest, without requiring a steel of a yield stress of 355 MPa or higher, that is, the designs that do not excessively deform during the considered design impact. The approach used to calculate the maximum bending moment produced on a frame determines the resistance of the design (required yield stress). In this way, the assumptions for the most conservative (simply supported frames), optimistic (fixed frames) and realistic (averaged simply supported and fixed frames) supporting systems give a weight reduction, compared with that of the FSICR, of 14.2 %, 14.13 % and 13.31 % respectively. The lightest designs usually correspond with custom-built T designs. This occurs due to the greater variation in the parameters that can be made for this profile type, it leading to higher optimization. Furthermore, the most realistic value (average) has a maximum bending moment slightly higher than that for the most optimistic assumption. This means that most of the designs within both design spaces are the same, showing only minor changes in their ability to withstand the impact (resilience). This methodology may provide a tool to be used by ship designers in direct design of ice-going ships, and by Classification Societies to set the requirements needed for ice class vessels.

ACKNOWLEDGEMENTS

The authors acknowledge the Spanish Ministry for Economy and Competitiveness under Grants RTI2018-094744-A-C22 (NICESHIP), which have made it possible to present this research at the MARINE 2021 conference. Thanks to Simón Carrillo Segura, for his help and contributions to the research project.

REFERENCES

IMO (2014). International Code for Ships Operating in Polar Waters (POLAR CODE). International Maritime Organization. MEPC 68/21/Add.1.

TRAFI (2016). Ice Class Regulations and the Application Thereof. Finnish Transport Safety Agency.

Popov, Y. N., Faddeyev, O. V, Kheisin, D. E. & Yalovlev, A. (1967). Strength of ships sailing in ice (FSTC-HT-23.). Leningrad: Sudostroenie Publishing House, U.S. Army Foreign Science and Technology Center. (Translation 1969).

Daley, C.G. (2001). Oblique Ice Collision Loads on Ships Based on Energy Methods. Published in Ocean Engineering International, Vol.5, No.2, 67-72.

Jumeau M. & Riska K. (2018). Ice interaction with Ships. Calculation of the Ice Force in Collision with a Finite Ice Floe. Training report. Total, Centrale Nantes. Unpublished.

WMO (2014). Sea Ice Nomenclature. WMO No. 259, Volume 1 – Terminology and Codes; Volume II – Illustrated Glossary; III – International System of Sea-Ice Symbols. 5th Session of JCOMM Expert Team on Sea Ice.

Russian Maritime Register of Shipping (2016). Rules for the Classification and Construction of Sea-Going Ships. Part II. Hull.

Joensuu A. & Riska K. (1989). Structure/Ice Contact, Measurement Results from the Joint Tests with Wärtsilä Arctic Research Centre in Spring 1988. Helsinki University of Technology, Laboratory of Naval Architecture and Marine Engineering, Report M-88, Espoo, 1989.

Daley, C.G. (1991). Ice Edge Contact - A Brittle Failure Process Model. Acta Polytechnica Scandinavica, Mechanical Engineering Series No. 100, 92 pp. Published by the Finnish Academy of Technology, Helsinki.

Daley, C.G. (1999). Energy Based Ice Collision Forces. Port and Ocean Engineering under Arctic Conditions, POAC'99. Espoo, Finland.

Daley C.G. & Kim H. (2010). Ice Collision Forces Considering Structural Deformation. Proceedings of the ASME 2010 29th International Conference on Ocean, Offshore and Arctic Engineering. OMAE2010-20657. June 2010, Shanghai, China.

Bueno, A. (2012). Modeling Impact of Sea Ice on Ship and Offshore Structures. Ships Structures Committee. SSC-465.

Dolny, J. (2018). Methodology for Defining Technical Safe Speeds for Light Ice-Strengthened Government Vessels Operating in Ice. Ships Structures Committee. SSC-473.

Riska K. & Kämäräinen J. (2011). A Review of Ice Loading and the Evolution of the Finnish-Swedish Ice Class Rules. Society of Naval Architects and Marine Engineers.

ESL Shipping, 2020; https://www.eslshipping.com/fleet/ships/m-s-eira

Sanderson, T.J.O. (1988). Ice Mechanics - Risks to Offshore Structures. Published Graham and Trotman, London, 1988.

IACS (2019). UR I2: Structural Requirements for Polar Class Ships. Requirements concerning Polar Class. International Association of Classification Societies.

Hughes, O. F. & Paik, J. K. (2010). Ship Structural Analysis and Design. Society of Naval Architects and Marines Engineers (SNAME). Library of Congress Card Catalog. No. 88-62642. ISBN No. 978-0-939773-78-3.